# Residual Motion of Hemoglobin-Bound Spin Labels as a Probe for Protein Dynamics

Heinz-Jürgen Steinhoff, Klaus Lieutenant, and Jürgen Schlitter

Institut für Biophysik, Ruhr-Universität Bochum, D-4630 Bochum, Bundesrepublik Deutschland

Z. Naturforsch. **44c**, 280–288 (1989); received October 24, 1988

Protein Dynamic, Electron Paramagnetic Resonance, Spin Label, Hemoglobin, Hydration

The residual motion of spin labels bound to cysteine β93 of methemoglobin and oxyhemoglobin has been analyzed as a function of temperature and hydration. The rotational diffusion of the whole protein molecule has been prevented or restricted by crystallization, lyophilization or by high viscosity of the solution. The residual motion of the labels is characterized by an angle of the limited motion cone and their rotational correlation time using computer simulations of the EPR spectra. Two types of motion can be separated due to different correlation times and different dependences on temperature and hydration. One of these motional mechanisms can be shown to be determined by protein fluctuations. Correlation times of these fluctuations decrease from $2 \times 10^{-8}$ s at $T = 220$ K to $10^{-9}$ s at $T = 300$ K in the samples of high water concentration. Strong correlation between the properties of the hydration shell and these fluctuations are observed.

## Introduction

Evidence for internal motions in globular proteins reflecting the presence of molecular flexibility has come from a number of different experimental approaches that include for example Mössbauer spectroscopy [1–3], X-ray crystallography [4, 5], electron paramagnetic resonance (EPR) [6, 7], and fluorescence spectroscopy [8]. Internal flexibility of proteins may be relevant to the mechanisms of allosteric transitions, protein folding and enzymatic activity. Using the spin label technique, an attempt is made to adduce informations about the protein surface dynamic, for example the mobility of amino acid side chains, and how this dynamic is influenced by hydration and temperature.

A nitroxide spin label covalently bound to a protein can be regarded as an artificial amino acid side chain. The EPR spectrum of this label is sensitive to the rate of nitroxide rotational motion. So the EPR spectrum of a bound spin label should directly reflect the motion of the macromolecule itself or some residual motion of the label with respect to the whole macromolecule. In the present investigation the protein molecule is immobilized by crystallization, by lyophilization, or by addition of sucrose to the protein solutions so that the rotational diffusion of the whole molecule is prevented or restricted so that it has no effect on the EPR spectrum. Our aim in this paper is to extract informations about the residual motion of the spin label from the EPR spectrum and to investigate the dependence of this motion on temperature and hydration.

For this purpose the EPR spectra of the labels 4-maleimido-2,2,6,6-tetra-methylpiperidinyl-1-oxyl (Mal6), 3-maleimido-2,2,5,5-tetramethyl-3-pyrrolidinyl-1-oxyl (Mal5) and N-(1-oxyl-2,2,6,6-tetramethyl-4-piperidinyl)iodoacetamide (JAA6) bound to Cys β93 of methemoglobin (metHb) or oxyhemoglobin ($HbO_2$) are analyzed. Mal5, Mal6 and fractions of JAA6 labels occupy the tyrosine pocket of this protein molecule providing a label position inside the molecule [10].

Johnson [6] has shown that the labels Mal5 and Mal6 exhibit motional fluctuations which have been detectable for desalted hemoglobin at approximately 258 K using saturation transfer techniques and at approximately 298 K using line width measurements of normal absorption spectra. Using ELDOR methods, Hyde *et al.* [11] have also shown the existence of significant librational motion effects for Mal6 labeled $HbO_2$ frozen in ice at about 263 K. In a preceding paper [12] one of us has demonstrated that the strong decrease of the hyperfine splitting of JAA6 labeled methemoglobin samples above 200 K must be due to motional fluctuations of the label.

In the present communication, a computer model is applied to simulate the influence of librational motion on EPR spectra. Rotational correlation times of the residual label motion are deduced from the spectra and it is carefully checked that the observed fluc-

Reprint requests to H.-J. Steinhoff.

Verlag der Zeitschrift für Naturforschung, D-7400 Tübingen
0341–0382/89/0300–0280 $ 01.30/0

tuations are due to fluctuations of the protein conformation. Additionally the rotational correlation behavior of 2,2,6,6-tetramethyl-4-oxopiperidine-1-oxyl (Tempone), which had penetrated into methemoglobin single crystals was investigated to get informations about the water of crystallization and its properties close to the protein surface.

## Methods

### *Materials and equipment*

Oxyhemoglobin was prepared from fresh horse blood samples by the methods of Benesch *et al.* [13]. Spin labeling (JAA6, Mal5, Mal6) of oxyhemoglobin followed the procedure of McCalley *et al.* [14]. The oxidation of the labeled oxyhemoglobin to methemoglobin was achieved by addition of a threefold amount of $K_3(Fe(CN)_6)$. The sample was desalted by running through a column of Sephadex G-25. Polycrystalline samples and single crystals were prepared by mixing the solutions of labeled metHb with buffered ammonium sulfate solutions according to the method of Perutz [15].

Hydrated samples were prepared by equilibrating lyophilized metHb at 25 °C in quartz tubes on a high vacuum line, connected with a flask containing a mixture of degassed sulfuric acid and water of known composition. The vapor pressure of these mixtures at different temperatures were taken from the literature [16]. The amount of sorbed water is given by the ratio of weight W% = g(water)/g(dry protein) × 100 and was calculated from sorption isotherms given in [17]. Sucrose solutions were prepared at about 4% (w/v) intervals from 48% to 64% using reagent grade sucrose. Solution viscosities were taken from Landolt-Börnstein [18].

EPR spectra were measured on a home-made X-band spectrometer equipped with a modified Oxford ESR 9 variable temperature accessory. The microwave power used was 0.1 mW, the modulation frequency was 52 kHz and the modulation amplitude $0.4 \times 10^{-4}$ T. The magnetic field was measured with a Bruker B-NM 12 instrumentation. 2,2-Diphenyl-1-picrylhydrazyl (DPPH) powder served as a $g$-value standard ($g = 2.0037$). After analog-digital conversion the spectra were recorded in a personal computer (CBM 8296, Commodore) and then transmitted to a Cyber 855 (Control Data).

### *EPR spectra analyzation*

Experimental EPR spectra were characterized by means of least square fittings of simulated spectra with a time-independent effective Hamiltonian [12]:

$$H = \beta_e S g H + S A I \tag{1}$$

where $H$ is the external field vector, $\beta_e$ the Bohr magneton, $S$ the electron spin operator, $I$ the nuclear spin operator, $g$ the electron $g$-value tensor and $A$ the electron nuclear hyperfine interaction tensor. Introducing molecular motion with correlation times less than $10^{-7}$ s the spectrum can be simulated by replacing the tensors $g$ and $A$ by spatial averaged effective tensors $g'$ and $A'$ and this yields a time-independent effective Hamiltonian $H_{\text{eff}}$. The validity of this effective Hamiltonian has been checked in the rotation correlation time range between $6 \times 10^{-7}$ s $> \tau > 10^{-10}$ s by least square fitting of generated powder spectra using $H_{\text{eff}}$ to spectra calculated using the stochastic Liouville method of Freed [19]. Parameters of the fitting procedure are the six principle values of the tensors $g'$ and $A'$. It could be shown that the deviation of the fitted TrA′ from the "true" value TrA is less than 1.5% for $S_z \geq 0.8$. This check is described in detail elsewhere [12]. The degree of averaging of the spectra is characterized by an order or averaging parameter $S_z$ defined as

$$S_z = \frac{A_{zz}' - 1/3\ \mathrm{TrA}'}{A_{zz} - 1/3\ \mathrm{TrA}} \tag{2}$$

The tensor parameters without primes are the rigid limit values. $S_z$ will change from 1 for the rigid limit case, $A' = A$, to zero in the case of complete averaging. In the following the experimental EPR spectra are characterized in terms of $S_z$ and TrA′. All calculations and spectra simulations were executed on a CYBER 855 computer.

## Results

### *Methemoglobin labeled with Mal6 or Mal5*

The behavior of the parameter $S_z$ and of the trace of the hyperfine tensor 1/3 TrA, with temperature for the crystallized and lyophilized samples is shown in Fig. 1. The values $S_z$ of all samples decrease with increasing temperature. Above 190 K the rate of change of $S_z$ of the wet samples is greater than that of the dry sample. But the trace of the hyperfine tensors of all samples is independent of temperature in the whole temperature range investigated even in the

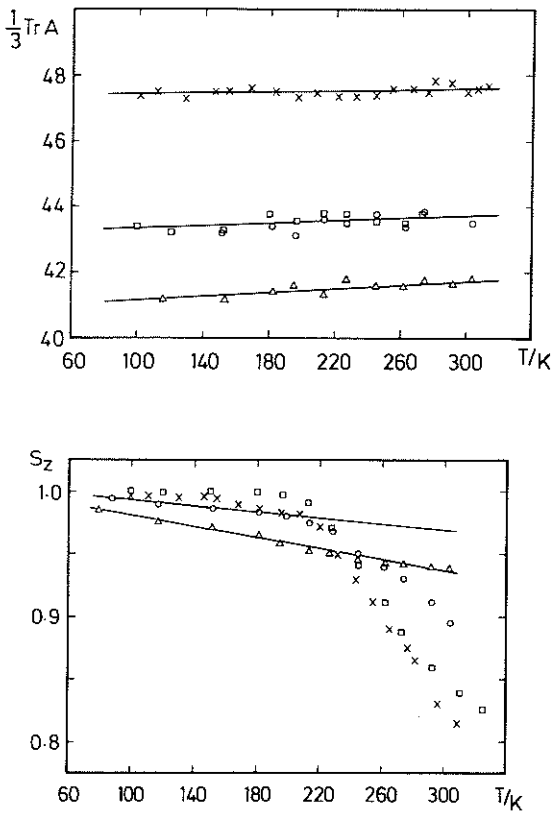


Fig. 1. a) The trace of the hyperfine tensor, 1/3 TrA, as a function of temperature of spin-labeled methemoglobins: (□) crystallized metHb-Mal5; (△), lyophilized metHb-Mal5, degree of hydration W% = 0; (○), lyophilized metHb-Mal5, W% = 16.3; (×) crystallized metHb-Mal6. b) The parameter $S_z$ as a function of temperature for the samples shown in a). The lines are the best fits of the torsional oscillation model to the lyophilized metHb-Mal5 data.

temperature range between 190 and 300 K. However, the hyperfine separation as well as 1/3 TrA of the lyophilized metHb-Mal5 sample is less than the corresponding values of the wet samples. It is known that the value of the trace of the hyperfine tensor is a criterion for the polarity of the label environment, and it could be shown that the values of 1/3 TrA and $A_{zz}$ for spin labels in environments of different polarity are correlated [12]. So the difference of the values of 1/3 TrA of the different metHb-Mal5 samples are due to different environmental polarities the labels are exposed to. On the other hand, the independence of the trace of $A$ from temperature is strong evidence that the temperature-induced change of the tensor element $A_{zz}$ and of $S_z$, especially in the temperature range above 200 K, is not due to temperature-induced changes of the polarity but must be due to changes in motional freedom.

A simple model for anisotropic motional fluctuations is to allow the molecular $z$-axis of the attached spin label to execute limited amplitude oscillations. Plausible mechanisms of label motions include inversion of the N–O bond with respect to the C–N–C plane within the six-membered nitroxide ring or torsional oscillations of the nitroxide ring about the C–N bond between this ring and the leg of the label [6, 7]. Each of these mechanisms will produce transient reorientation of the nitroxide principle $z$-axis with respect to the external magnetic field. In the first step we shall assume that these torsional oscillations are of high frequency ($\tau_c < 10^{-10}$ s) [4]. This can be expressed by partial averaging of the $A_{zz}$, $A_{yy}$ and $A_{xx}$ hyperfine tensor elements. Since there is nearly axial symmetry of the hyperfine matrix of the spin labels used here we may apply the formulas derived by Van *et al.* [20] for the oscillation model setting $A_{xx} = A_{yy} = A_\perp$. The relation between the elements of the rigid limit tensor $A$ and the motional averaged parameters $A_{zz}(\varphi)$ yields:

$$A_{zz}(\varphi) = A_\perp + (A_{zz} - A_\perp) \times 1/2 \times (1 + P)$$
$$\text{where } P = \sin\varphi \cos\varphi/\varphi. \quad (3)$$

A temperature dependence in the oscillation amplitude will produce a temperature-dependent hyperfine separation. We consider the steric restriction of the label binding site as being equivalent to an energy barrier $E_a$, which hinders full 180° rotational motion of the nitroxide ring about the C–N bond between the nitroxide and the "leg". As an approximation, we assume the potential well to be of the form [4]

$$U = E_a(1 - \cos^2\theta). \quad (4)$$

For small amplitude motion the dependence of $\varphi$ on temperature is given by [4]

$$\varphi(T) = (RT/E_a)^{1/2}. \quad (5)$$

Least square fits of Eqn. (3) and (5) to the experimental values $A_{zz}(T)$ yield the rigid limit parameters $A_{zz}$ and the energies $E_a$. The parameters $E_a$ are given in Table I, the fits are shown as lines in Fig. 1. The results indicate that this model is a good description of the temperature dependence of $A_{zz}(\varphi)$ and $S_z$ for the lyophilized dry sample in the whole temperature range shown and for the wet samples with a high

Table I. Energy barrier $E_a$ (oscillation model) fitted with a high temperature cut off at $T = 200$ K.

| Sample | metHb-Mal5 | metHb-Mal5 | metHb-Mal5 | metHb-Mal6 |
|---|---|---|---|---|
| | W% = 0 | W% = 16.3 | crystallized | crystallized |
| $E_a$/kJmol$^{-1}$ | 19.0 ± 0.7 | 37.0 ± 2.0 | 42 ± 10 | 31.0 ± 5.0 |

temperature cut off at $T = 200$ K. The semiangle of oscillation may be calculated from the experimentally determined values of $S_z$ using Eqn. (2) and (3). It holds:

$$P = 4/3\, S_z - 1/3 \tag{6}$$

with $P$ defined in Eqn. (3).

For the lyophilized dry system, the assumption of a constant $E_a$ is probably reasonable and the model is adequate to fully explain the observed temperature dependence of this system. However, the strong decrease of $S_z$ for all water-containing samples above 200 K cannot be described by this model with a temperature-independent potential energy barrier $E_a$. In frozen aqueous systems, there is evidence that the ice structure around the protein will produce strong suppression on the nitroxide librational motion. The values of $E_a$, determined for these systems up to 200 K, are significantly greater than that of the lyophilized, dry sample (*cf.* Table I). As the temperature increases and the ice structure around the protein relaxes, the protein flexibility will increase, which would probably lead to an increase of the amplitude of librational motion. This mechanism could explain the changes of the EPR spectra between 200 and 260 K but it is no explanation for the behavior of $S_z$ with temperature above the melting-point of water.

Since the presence of water at the surface of the protein seems to be an essential condition for the changes of the EPR spectra above 200 K, a second mechanism for the spectral changes has to be discussed. Adsorbed water in myoglobin single crystals is found to exhibit a fast increase of the relaxation rate with temperature between 200 K and 300 K [1]. Investigations of methemoglobin single crystals [21] show a similar behavior of the protein-bound water. Correlations between conformational fluctuation rates of the protein as measured by Mössbauer spectroscopy and the relaxation rate of adsorbed water have been evaluated. So the observed changes of $S_z$ above 200 K may be due to the change of frequency of slow motional fluctuations of the label in a limited motion cone.

So we drop the restriction of high frequency oscillations and take into account not only the semiangle of oscillation but also the rate of oscillation. A simple model is to allow the molecular $z$-axis of the bound label to jump between two orientations with respect to the external magnetic field characterized by the semiangle $\theta$ with a rate $r$. The theory of EPR spectra simulations on the basis of this model is given in the appendix.

Several spectra simulated using values of $\tau = 1/(6r)$ in the range $10^{-10}$ to $10^{-7}$ s are given in Fig. 2 for different semiangles $\theta$. As the rate of the oscillation and the semiangle increase, the separation between the outer extrema ($2\,A_{zz}$) decreases, a consequence of motional averaging of the hyperfine anisotropy in the plane perpendicular to the oscillation axis of the spin probe. The degree of motional averaging of the simulated spectra is again characterized by the parameter $S_z$ (Eqn. (2)). For three angles $\theta$ the behavior of $S_z$ with correlation time $\tau$ is given in Fig. 3. Additionally the $S_z$ values for isotropic Brownian diffusion are shown. This curve was determined from the fittings of spectra calculated on the basis of the time-independent effective Hamiltonian Eqn. (1) to spectral simulations using the exact stochastic Liouville method of Freed [19]. All curves show a similar behavior of $S_z$ with the steepest descent between $10^{-9}$ and $10^{-8}$ s independent of the semiangle $\theta$. For values of $\tau$ less than $10^{-11}$ s $S_z$ shows an asymptotic behavior with boundary values $S_z(0)$ depending on $\theta$. In the range $10^{-10} < \tau < 5 \times 10^{-8}$ s $\tau$ can be calculated from the observed values of $S_z$ using the empirical relationship

$$\tau = 2.27 \left\{ \frac{S_z - S_z(0)}{1 - S_z} \right\}^{0.87} \text{ns}. \tag{7}$$

If we assume an activation process to describe the temperature dependence of the rate of oscillation, the term $\tau$ in Eqn. (7) has to be replaced by

$$\tau = \tau_0 \exp(-\Delta H^*/RT) \tag{8}$$

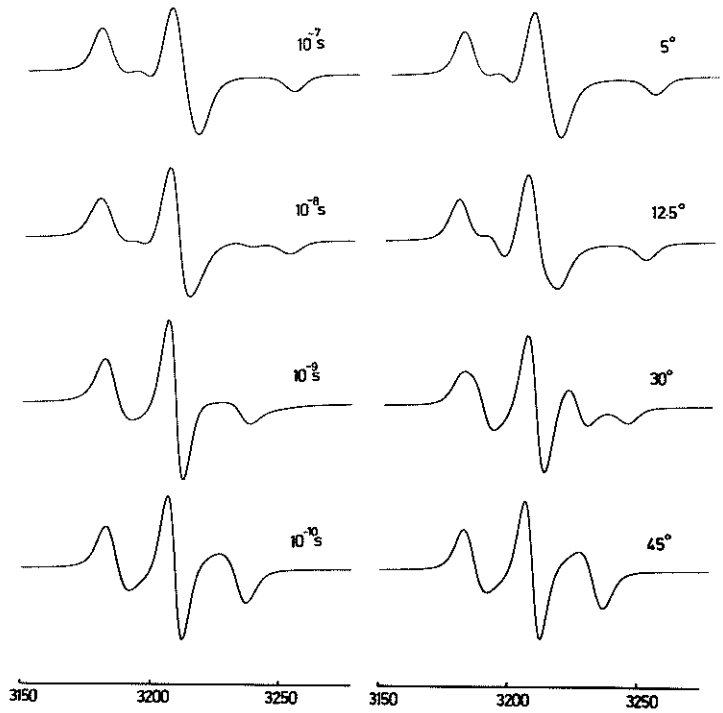


Fig. 2. EPR spectra simulations using the two-jump model (*cf.* appendix). (Left), semiangle of the limited motion cone $\theta = 45°$ and different correlation times; (right), correlation time $\tau = 1.7 \times 10^{-11}$ s and different semiangles. Other parameters of the simulation are: $A_{xx} = 7.4$ G, $A_{yy} = 6.5$ G, $A_{zz} = 37.1$ G, $g_{xx} = 2.010$, $g_{yy} = 2.006$, $g_{zz} = 2.002$, $T_2^{-1} = 2.5$ G.

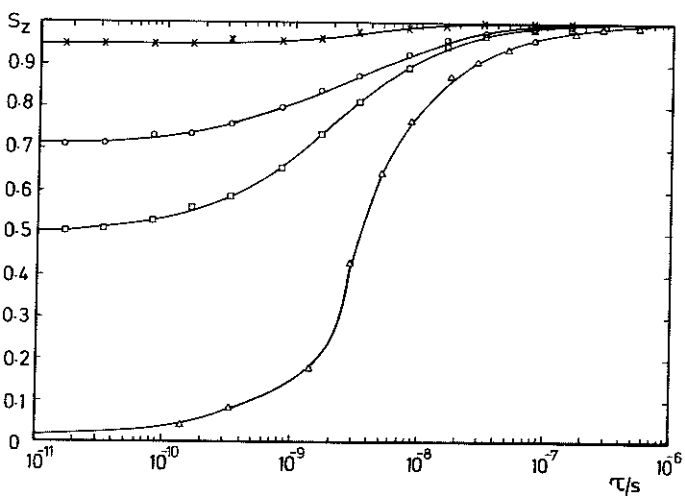


Fig. 3. The parameter $S_z$ *versus* correlation time for the two-jump model: (×), semiangle $\theta = 12.5°$; (○), $\theta = 30°$; (□), $\theta = 45°$; and for (△) isotropic Brownian diffusion. This curve was determined from fittings of spectra on the basis of the time-independent effective Hamiltonian to spectral simulations using the stochastic Liouville equation [19]. Parameters of the simulations are given in [12].

and Eqn. (7) may be fitted to the experimental values given in Fig. 1 to get the parameters $\tau_0$, $\Delta H^*$ and $S_z(0)$, which are assumed to be temperature-independent in the temperature range considered. The values of $\tau$ have then been calculated using Eqn. (7) with the experimental values of $S_z$ and the fitted values of $S_z(0)$.

Arrhenius plots are given in Fig. 4. Within experimental error there is no deviation from linear dependence in the plots illustrated. The behavior of the correlation times for the polycrystalline metHb-Mal6 and metHb-Mal5 samples with temperature is identical within experimental error. The enthalpy of activation for the fluctuations of these labels determined from the slope of the regression curve is found to be 19.0 ± 1.0 kJ/mol. However, these two systems differ slightly in the boundary value $S_z(0)$ and therefore in the semiangle of oscillation. We get $\theta = 30°$ for the Mal6 system and $\theta = 27°$ for the Mal5 system. The Arrhenius plot of the lyophilized metHb-Mal5 with a hydration degree W% = 16.3 shows also linear behavior. The enthalpy of activation was calculated to 17.8 ± 2.0 kJ/mol and is identical with the value of the polycrystalline samples within experimental error. However, the values of $\tau$ are less than those of the polycrystalline samples in the whole temperature range investigated, reflecting a higher degree of restriction of this kind of label motion in the hydrated lyophilized sample. With a degree of hydration substantially less than W% = 8 (unpublished results) this kind of motion is not visible any more in the EPR absorption spectra. Since spectral changes are detectable if $\tau$ is less than $10^{-7}$ s, the disappearance of these changes is evidence that the correlation times of the fluctuations in these lyophilized samples exceed $10^{-7}$ s.

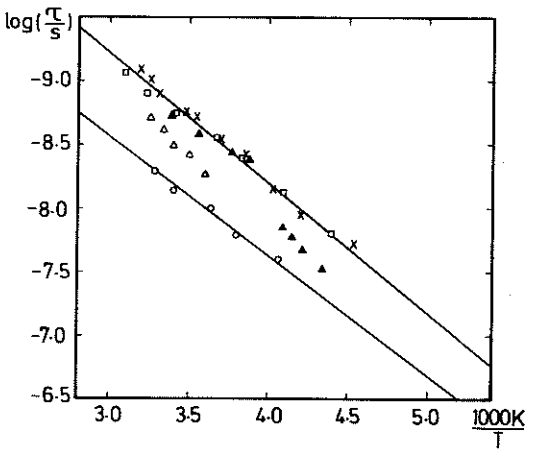


Fig. 4. Arrhenius plots of the label fluctuations: (□), crystallized metHb-Mal5, $S_z(0) = 0.78$; (○), lyophilized metHb-Mal5, W% = 16.3, $S_z(0) = 0.78$; (×), crystallized metHb-Mal6, $S_z(0) = 0.73$; (△), metHb-JAA6 in viscous solution ($\tau$ determined from the outer hyperfine separation using Eqn. (7) and (2) with $S_z(0) = 0.73$); and (▲), free Tempone radicals in metHb single crystal, $\tau$ determined from the calibration curve for isotropic rotational diffusion given in Fig. 3.

*Oxyhemoglobin labeled with JAA6*

The observed label fluctuations are not unique to polycrystalline or hydrated lyophilized Mal-labeled hemoglobins. As an example the correlation times of JAA6-labeled $HbO_2$ in solution have been determined. By addition of sucrose to the solution the viscosity has been increased to an amount that the rotational diffusion of the whole hemoglobin molecule has a negligible effect on the EPR spectra. This has been checked by extrapolation of the $S_z$ *versus* $T/\eta$ curves to infinite viscosity ($T/\eta = 0$).

In $HbO_2$-JAA6 samples, two orientations of the spin label with respect to the whole molecule have been identified [22]. One of these orientations extends into the tyrosine pocket and the orientation found is identical to that of Mal5 and Mal6 labels [10]. The spectral components corresponding to this fraction of JAA6 labels may be separated from the whole EPR spectrum due to the strong immobilization and the resulting higher hyperfine separation compared to the weakly immobilized components. The correlation times of the strongly immobilized fraction of JAA6 are shown in Fig. 4. We can recognize a very similar behavior of the correlation times of the label fluctuations in this sample compared to those of the polycrystalline metHb-Mal5 and metHb-Mal6 samples. The slight difference between the values of $\tau$ of the two sets of samples might be due to the different labels and different conformational environments of the label-binding sites.

*Unbound radicals diffused into methemoglobin single crystals*

The water content of metHb single crystals is 52% [23] consisting of bound water and bulk water. The influence of this water of crystallization on the rotational fluctuations of small molecules will give further information about the labels fluctuations. For

this purpose we investigated metHb single crystals into which tempone radicals have diffused. These radicals did not react with the protein within the time of investigation and we got an isotropic spectrum independent from the orientation of the crystal with respect to the external magnetic field. So the radicals are assumed to rotate freely and deliver informations about the local viscosity. The rotational correlation times of the radicals were determined using the calibration curve for $S_z(\tau)$ for isotropic Brownian rotational diffusion. In the whole temperature range the rotational correlation times of the free and the bound labels are correlated (*cf.* Fig. 4). Above 260 K (1000 K/$T$ = 3.9) the values of rotational correlation times of the free radicals equal almost those of the bound labels. The discontinuity found for $\tau(T)$ of the free radicals at 260 K may be explained by melting of the bulk water inside the crystals. Above this temperature the intermolecular water cavities are an additional solute volume for the unbound radicals and the overall rotational correlation time decreases. These results have been achieved with crystals in a water-saturated atmosphere. On drying the crystals the rotational correlation times of the free and of the reacted labels increase in the same manner.

## Discussion

*Mechanisms of label motion within the protein matrix*

Johnson has discussed several possible mechanisms of label motion within the protein matrix [6] which include a) ring conformational transitions between "boat" and "chair" conformations or between two possible "twisted" ring conformations, or inversion of the N−O bond with respect to the C−N−C plane within the nitroxide ring, b) torsional oscillations of the nitroxide ring about the C−N bond between the Tempo and the maleimide moieties of the label, and c) protein structural fluctuations which affect the label conformation and orientation within the protein. We consider now how far the librational mechanisms listed above are compatible with our experimental results.

a) A ring conformational transformation between the "boat" and "chair" forms would be to reorient the principle $x$- and $z$-axes by 104° while the transformation between the two twisted forms would produce a 50° reorientation of the axes [6, 24]. These are much larger angles than are actually observed. Data from EPR crystallographic studies of Mal6-labeled horse Hb suggest that the Mal6 nitroxide ring probably exhibits only one ring conformation within its binding site [25]. Inversion of the N−O bond about the C−N−C plane would reorient both the principle $x$- and $z$-axes by approximately 35° in the six-membered ring and less than 7° in the five-membered ring [24]. The experiments show identical behavior of the relaxation rates above 200 K and similar angles of oscillation for both the six- and five-membered rings in the polycrystalline samples. Thus it appears unlikely that ring conformational transitions contribute significantly to the motional mechanisms observed here.

b) Since the rigidly bound nitroxide rings should be quite analogous to sterically hindered tyrosine rings, theoretical results concerning the dynamics of tyrosine side chains in proteins should be considered. The frequency of torsional oscillations of tyrosine rings are found to be in the range $10^{12}$ to $10^{13}$ $s^{-1}$ [26]. The root mean square fluctuations of the torsion angle and the torsion axes will be temperature-dependent and are found to be between 9° and 38° at $T$ = 308 K. These torsional oscillations seem to be adequate to describe the temperature dependence of the EPR spectra of the lyophilized dry sample and of the water-containing samples up to 200 K as discussed above. However, for the fluctuation mechanism observed above 200 K the correlation times of the wet samples differ from those predicted for torsional oscillations by about 4 orders of magnitude, so this mechanism alone does not fully explain the experimental results.

c) Thermally induced fluctuations in protein conformation might also affect the conformation of the label-binding site. These conformational fluctuations might change the orientation of the label or modulate the intramolecular modes of label motion, for example the torsional oscillations discussed in b). From Mössbauer spectroscopy of the heme iron of myoglobin [3] and from investigations of myoglobin by Rayleigh scattering of Mössbauer radiation [2] we know that protein specific intramolecular movements with $\tau < 10^{-7}$ s become visible above a characteristic temperature of typically 200 K. A similar behavior is seen here for the fluctuations of the label in the tyrosine pocket with $\tau = 10^{-7}$ s at $T$ = 190 K independent of the type of spin label used. Thus, this type of motion can be well explained by fluctuations in protein conformation.

*Influence of temperature and hydration*

From the above results we may separate between two types of motion, which are influenced by temperature and hydration in a different manner. A fast vibration of the label ($\tau < 10^{-12}$ s) within a limited motion cone determines the behavior of the EPR spectra of the dry protein in the whole temperature range investigated. On addition of water to the protein the potential barrier characterizing this vibration increases (*cf.* Table I). Simultaneously a second type of motion becomes visible, which we assign to fluctuations of the protein conformation. This process is strongly influenced by the properties of the hydration shell. An increase of the water concentration leads to an increase of the fluctuation rate. A similar behavior of motion was reported for spin-labeled ribonuclease [27]. On varying the temperature from 220 K to 300 K the correlation times of the fluctuations decrease from $2 \times 10^{-8}$ s to $10^{-9}$ s in the samples of high water concentration (polycrystalline, viscous solution). Similar behavior of the correlation times of free radicals rotating isotropically close to the surface of the protein and the anisotropic motion of the labels inside the protein are an additional indication of a strong interaction between the dynamical properties of the water surrounding the protein and the protein fluctuations. The dependence of these fluctuations on viscosity will be subject of a forthcoming study.

## Appendix

*EPR spectrum of a two-jump model*

A general description of the quantum mechanical spin motion under the influence of a stochastically modulated Hamiltonian $H$ is given by the stochastic Liouville equation [28]

$$\dot{\varrho}(\Omega,t) = i/\hbar\,[H(\Omega,t), \varrho(\Omega,t)] - \Gamma\,\varrho(\Omega,t) \quad (A1)$$

for the spin density matrix $\varrho$. The underlying stochastic process is described by the Markoff operator $\Gamma$ acting on the stochastic variable $\Omega$.

For a two-jump model, $\Omega$ is replaced by an index $\alpha$ taking the values 1 or 2 and denoting the two possible states of the spin environment. The Hamiltonian is

$$H_\alpha(t) = H_\alpha + \varepsilon(t) \quad (A2)$$

where $H_\alpha$ is the proper spin Hamiltonian, Eqn. (1) and $\varepsilon(t)$ the interaction with the microwave field. $\Gamma$ then becomes a $2 \times 2$ matrix defined by the jumping rates which, for the sake of simplicity, are both assumed to be $r$. $H_\alpha$ and $\Gamma$ define a time-independent equilibrium density matrix

$$\bar{\varrho}_\alpha = \exp(-H_\alpha/kT)/N \sim (1 - H_\alpha/kT)/N \quad (A3)$$

for vanishing $\varepsilon(t)$, $N$ being a normalization factor. $\bar{\varrho}_\alpha$ is used to reformulate the stochastic Liouville equation of the two-jump model as

$$\begin{pmatrix} \dot{\varrho}_1 \\ \dot{\varrho}_2 \end{pmatrix} + \frac{i}{\hbar}\begin{pmatrix} [H_1, \varrho_1] \\ [H_2, \varrho_2] \end{pmatrix} + \begin{pmatrix} r + T_2^{-1} & -r \\ -r & r + T_2^{-1} \end{pmatrix}\begin{pmatrix} \varrho_1 \\ \varrho_2 \end{pmatrix} = \begin{pmatrix} [\varepsilon, \bar{\varrho}_1] \\ [\varepsilon, \bar{\varrho}_2] \end{pmatrix}\left(-\frac{i}{\hbar}\right). \quad (A4)$$

A rotationally invariant line width $T_2^{-1}$ is inserted to allow for further broadening due to other mechanisms. Solving Eqn. (A4) requires in general a large amount of numerical calculations since there will be no set of basis vectors diagonalizing $H_1$ and $H_2$ simultaneously. A simple and numerically fast solution which is essential for the application to spectral simulations and fits can be found in cases where the two states differ only so little that the Hamiltonians can be considered as diagonal in the same optimum basis. On this assumption there is no coupling among the possible transitions and Eqn. (A4) can be solved analytically. The spin Hamiltonian, Eqn. (1), yields three transition frequencies depending on the nuclear spin projection $M = -1$, 0, and 1 and the Euler angles $\theta$ and $\varphi$ describing the orientation of the tensor principle axes in the laboratory system. The explicite form of $\omega_M(\theta,\varphi)$ basing on the approximation of Libertini and Griffith [29] is given elsewhere [12].

In order to define our two-jump model, we assume that at each average orientation $\{\theta, \varphi\}$ of the spin label – which is fixed by the orientation of the macromolecule – the label itself can take two states with $\{\theta \pm \Delta\theta, \varphi\}$. The resulting transition frequencies entering the spin equation of motion are hence

$$\omega_{M\alpha} = \omega_M(\theta \pm \Delta\theta, \varphi). \quad (A5)$$

The interaction of the electron spin with the microwave field,

$$\varepsilon(t) = 1/2\,\beta_e H_1[S_+ \exp(-i\omega t) + S_- \exp(i\omega t) \quad (A6)$$

leads to a power absorption

$$P \propto \int \sin\theta\, d\theta\, d\varphi\; 1/2 \sum_{\alpha,M} Im\,\{Z_{\alpha,M}(\theta,\varphi)\} \quad (A7)$$

where $Z_{\alpha,M}$ is the Fourier transform at frequency $\omega$ of the transition matrix element $<M-½|\varrho_\alpha|M+½>$. One therefore has to transform Eqn. (A4) into an equation for $Z_\alpha$ and obtains, by neglecting saturation terms,

$$Z_{\alpha,M} \propto \frac{\omega - \omega_{M\beta} - i(T_2^{-1} + 2r)}{[\omega - \omega_{M1} - i(T_2^{-1} + r)][\omega - \omega_{M2} - i(T_2^{-1} + r)] + r^2} \quad (A8)$$

where $\beta = 2$ for $\alpha = 1$ and *vice versa*.

The resulting line shape at a given orientation $\{\theta, \varphi\}$ is in formal agreement with the one derived from the classical Bloch equations for a two-jump model of chemical exchange [30]. The textbook example gives a good idea of the influence of the jumping rate $r$. At small rates $r$ either state arises as a separate resonance line in the spectrum which hence becomes an ordinary powder spectrum. With increasing rate, however, the two peaks broaden and finally collapse into a single line. Only at intermediate rates $r \sim |\omega_{M1} - \omega_{M2}|$ the spectrum is sensitive to the rate and, due to the dependence of the $\omega_{M\alpha}$ on the jumping angle $\Delta\theta$, also to the geometrical changes connected with the rate process.

*Acknowledgement*

Special thanks are due to Prof. A. Redhardt who supported this work with numerous inspiring conversations.

[1] G. P. Singh, F. Parak, S. Hunklinger, and K. Dransfeld, Phys. Rev. Lett. **47,** 685–688 (1981).
[2] Yu. F. Krupyanskii, F. Parak, V. I. Goldanskii, R. L. Mössbauer, E. E. Gaubmann, H. Engelmann, and I. P. Suzdalev, Z. Naturforsch. **37c,** 57–62 (1982).
[3] F. Parak and E. W. Knapp, Proc. Natl. Acad. Sci. U.S.A. **81,** 7088–7092 (1984).
[4] H. Frauenfelder, G. A. Petsko, and D. Tsernoglou, Nature **280,** 558–563 (1979).
[5] D. Ringe and G. A. Petsko, Prog. Biophys. Molec. Biol. **45,** 197–235 (1985).
[6] M. E. Johnson, Biochem. **17,** 1223–1228 (1978).
[7] M. E. Johnson, Biochem. **20,** 3319–3328 (1981).
[8] J. Oton, E. Bucci, R. F. Steiner, C. Fronticelli, D. Franchi, J. Montemarano, and A. Martinez, J. Biol. Chem. **256,** 7248–7256 (1981).
[9] J. L. Finney, J. M. Goodfellow, and P. L. Poole, The Structure and Dynamics of Water in Globular Proteins, in: Structural Molecular Biology (D. B. Davies, W. Saenger, and S. S. Danyluk, eds.), p. 387, Plenum Press, New York 1982.
[10] J. K. Moffat, J. Mol. Biol. **55,** 135–146 (1971).
[11] J. S. Hyde, M. D. Smigel, L. R. Dalton, and L. A. Dalton, J. Chem. Phys. **62,** 1655–1677 (1975).
[12] H. J. Steinhoff, J. Biochem. Biophys. Meth. **17,** 237–248 (1988).
[13] R. E. Benesch, R. Benesch, R. D. Renthal, and N. Maeda, Biochem. **11,** 3576 (1972).
[14] R. C. McCalley, E. J. Shimshick, and H. M. McConnell, Chem. Phys. Lett. **13,** 115–119 (1972).
[15] M. F. Perutz, J. Cryst. Growth **2,** 54–57 (1968).
[16] J. Timmermans, in: Physico Chem. Constants, **Vol. IV,** New York 1960; D'Ans-Lax, in: Taschenbuch für Chemiker und Physiker, Springer Verlag, Berlin 1967.
[17] M. Kent and W. Meyer, J. Phys. D. **17,** 1687–1698 (1984).
[18] Landolt-Börnstein, Springer Verlag, New York, Heidelberg, Berlin 1950.
[19] J. H. Freed, in: Spin Labeling Theory and Applications (L. J. Berliner, ed.), pp. 53–132, Academic Press, New York 1976.
[20] S. P. Van, G. B. Birrell, and O. H. Griffith, J. Magn. Res. **15,** 444–459 (1974).
[21] W. Daseler, Dissertation, Ruhr-Universität Bochum, Bochum, F.R.G. 1987.
[22] H. M. McConnell, W. Deal, and R. T. Ogata, Biochem. **8,** 2580–2585 (1969).
[23] R. C. Ladner, E. J. Heidner, and M. F. Perutz, J. Mol. Biol. **114,** 385–414 (1977).
[24] J. Lajzerowicz-Bonneteau, in: Spin Labeling Theory and Applications (L. J. Berliner, ed.), pp. 239–249, Academic Press, New York 1976.
[25] J. C. W. Chien, J. Mol. Biol. **133,** 385–398 (1979).
[26] J. A. McCammon, P. G. Wolynes, and M. Karplus, Biochemistry **18,** 927–942 (1979).
[27] H. Janzen, E. Matuszak, E. v. Goldammer, and H. R. Wenzel, Z. Naturforsch. **43c,** 285–293 (1988).
[28] R. Kubo, J. Phys. Soc. Jap. Suppl. **26,** 1–5 (1969).
[29] L. J. Libertini and O. H. Griffith, J. Chem. Phys. **53,** 1359–1367 (1970).
[30] A. Carrington and A. D. McLachlan, Introduction to Magnetic Resonance, Harper & Row, New York 1969.